1.4 THE EFFECTS OF SURFACE HETEROGENEITY ON BOUNDARY-LAYER STRUCTURE AND ENERGY FLUXES FROM AIRCRAFT

M.A. LeMone, [1*] R.L. Grossman,[2] F. Chen,[1] K. Davis,[3] and B. Geerts[4]

[1]National Center for Atmospheric Research, Boulder, CO
[2]Colorado Research Associates, Boulder, CO
[3]Department of Meteorology, Penn State Univ., State College, PA
[4]Department of Atmospheric Science, Univ. of Wyoming, Laramie

1. INTRODUCTION

One of the goals of the International H_2O Project (IHOP) is to determine the effects of the land surface on the water-vapor field and on the initiation and evolution of storms. The land surface influences the water vapor field through its controls in evaporation and boundary layer (BL) growth. Through a number of mechanisms, the land surface can create or modulate circulations that are favorable for storm initiation or that can influence storm propagation.

We will use a combination of aircraft and surface data to determine how the land surface affected boundary-layer heterogeneity during IHOP. These data will be used to evaluate surface-layer and BL parameterization schemes. Companion talks in this session focus on the surface data and the use of the IHOP data in creating surface flux fields and model testing. Here, we focus on the richness of the King Air dataset for which well-defined mesoscale horizontal heterogeneity was typical.

2. DATA COLLECTION

The three King Air tracks (Figure 1) were arranged along an east-west line to sample a large range of precipitation and vegetation. The tracks were laid out in advance, to enable us to fly 65 m above the surface. Along the tracks are located at least three surface flux stations (the radar track has four). The radar (or west) track was designed to fly close to the Homestead site, to enable comparisons and a rich dataset to look at boundary-layer structure and evolution. The east track, used in CASES-97 (LeMone et al. 2000), was repeated to enable us to compare the CASES and IHOP datasets.

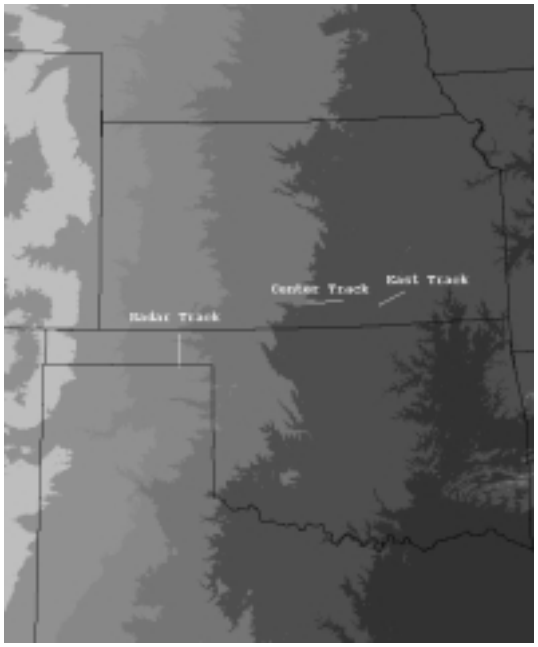

Fig. 1. Locations of the three Wyoming King Air BLH flight tracks. Lengths of tracks: East track: 41.4 km, Central track: 58.1 km, West (radar) track: 53.7 km.

Boundary-layer heterogeneity (BLH) flights were flown during fair weather conditions. Each flight pattern typically consisted of 10-15 straight and level legs above one of the three tracks, interspersed with soundings to sample the boundary layer top. Focus on a single track on each mission maximized sampling, and gave us the flexibility to pick the location with the best conditions. We flew two types of flight pattern. The first emphasized horizontal flux variability and involved seven or more straight-and level legs along a track at 65 meters above the surface (Figure 2). The second emphasized boundary-layer structure, and involved straight-and-level flight legs at 3-4 heights, ranging from 65 m to the upper BL, or on occasion just above the BL top. Vertical racetracks that alternated between 65 m

*Corresponding author address: Margaret A. LeMone, NCAR, PO Box 3000, Boulder, CO 80307; email: lemone@ucar.edu.

and some other height in the BL addressed both objectives.

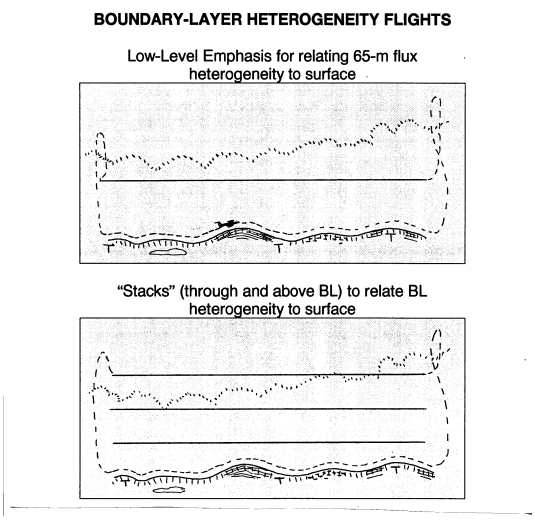

Fig. 2. Schematic the two types of BLH flight pattern. The "T"s in the figure denote flux towers.

Normally, the DLR Falcon or the NRL P-3 flew humidity-mapping missions to provide context for the King-Air BLH flights or for comparison purposes. On two occasions, the HRDL Doppler lidar was also functioning on the DLR Falcon. The S-Pol radar, the instruments at Homestead, and DOW radars often provided additional data for the BLH flights on the west track. More information on the supplementary data is provided in Weckwerth and Parsons (2003).

The University of Wyoming King Air is the ideal platform for such an effort. Its size minimizes disturbance to people and animals – vital when one is flying repeated low-level legs over a given region. Its flight level data provide us with accurate data on location, wind, temperature, and mixing ratio, and vertical fluxes of momentum and sensible and latent heat. Radiometric surface temperature and Normalized Differential Vegetation Index (NDVI) were also measured. The Wyoming mm-wavelength Cloud Radar (WCR) "sees" boundary-layer eddies primarily through Rayleigh scattering off insects; "visible" haze layers suggest that the small drops/large aerosols might have also been visible.

3. RESULTS AND DISCUSSION

The Table summarizes the 15 Wyoming King-Air BLH flights (there were two sorties on 6 June), based on the flight notes, King-Air flight legs and soundings, surface flux station data, and satellite images. There were numerous days with clear skies. Winds were mainly from the south, and speeds varied from nearly calm on 16 July to 13.2 m s^{-1} on 19 May. There is horizontal variability in potential temperature Θ on every mission: the range in mesoscale Θ–variability reached 1 K on some occasions. Variability in mixing ratio q was also frequent. The variability sometimes carried over into horizontal along-track divergence; only obvious examples are included in the table.

There are several explanations in the literature as to the sources of BL heterogeneity and mesoscale circulations, namely:

1. Horizontal variability in soil moisture or vegetation (Anthes 1984, Han and Anthes 1988, Segal et al. 1989, Chen and Avissar 1994, Pielke et al. 1997)
2. Terrain (Walko et al. 1992, Krettenauer and Schumann 1989)
3. BL modulation by tropospheric gravity waves (Clark et al. 1986)
4. Cloud (Segal et al. 1986) or smoke shadows (Segal et al. 1989)
5. Differential advection

Figures 3 and 4 show that the three flight tracks sample a variety of surface conditions. The pressure altitude of the terrain-following aircraft at 65 m agl in Fig. 3 shows significant variability in elevation along all three flight tracks. The Normalized Differential Vegetation Index (NDVI), at the bottom of Fig. 3, shows low NDVI on the west track reflecting sparse vegetation; relatively high NDVI for the east track, reflecting lush green grass and trees along riparian zones and windbreaks; and intermediate NDVI and vegetation along the central track. Figure 4 shows considerable horizontal variation in precipitation totals.

Table: Weather conditions for King Air BLH Flights

	Western Track					Central Track				Eastern Track				
Criterion	19M	20M	25M	29M	7J	21M	31M	6J	16J	27M	30M	17J	20J	22J
Cloud Amount ++ = clear + = nearly clear - = few clouds	+	- (3, 10)	+	- (3,10)	++	-	++	++	++	-	++	+-	-	-
Haze							Y	Y			Y			Y
Wind direction at 60 m	177	158	133	191	199	161	186	202	70	161	159	201	162	179
Wind speed at 60 m	13.2	13.1	2.5	4.9	10.6	10.7	6.6	5.3	0.8	5.5	3.9	7.7	5.3	9.4
Horizontal Variability Θ	Y	Y	Y	Y	Y	Y	Y	Y	Y	Y	Y	Y	Y	Y
Horizontal Variability q*		Y	Y	Y		Y	Y-		Y	Y	Y	Y	Y	Y
Horizontal Variability u_s**		Y							Y			Y		Y

*Typically the moisture evolution is more complex than temperature evolution.

**us is along-track component of the wind. This was not systematically looked for, but most days seemed to have little along-track convergence, in contrast to CASES-97

The west track will be particularly useful for looking at soil-moisture effects. Alfieri and Blanken (2002) found that moisture fluxes were closely linked with soil moisture at site 10, the flux station they operated at the northern end of the track. Figure 4 shows that the radiometric surface temperature on 29 May was nearly independent of NDVI. Instead, the radiometric temperature was tied to soil moisture. Flight-level data on this day shows that the Θ is 1 K warmer over the dry north end of the track than over the wet south end, through the boundary layer. Further, both flight-level and WCR images indicate a deeper boundary layer at the north end fed by more energetic plumes. Fortuitously, this track also had the most horizontal variability in precipitation; but this is mainly due to a series of storms on 27 May that deposited over 80 mm of rain at the south end of the track but ~20 mm at the north end.

In contrast, NDVI (and hence vegetation) is more important on the east track. From Figure 4, radiometric surface temperatures are more strongly related to NDVI than on the other two tracks. During CASES-97 (LeMone et al. 2000), differences in vegetation greenness could be used to explain much of the horizontal variability in heat fluxes, but soil moisture effects showed up strongly in the temporal variation (Yates et al. 2001).

Cloud shadow seemed to affect the boundary layer on one day, and rapid BL growth at one end of the flight track led to lower mixing ratios in some instance, but the cause has not yet been determined. LeMone et al. (2002) documented an apparently terrain-induced mesoscale circulation over the east track during CASES-97.

Examples of horizontal variability in PBL structure and fluxes will be shown.

.

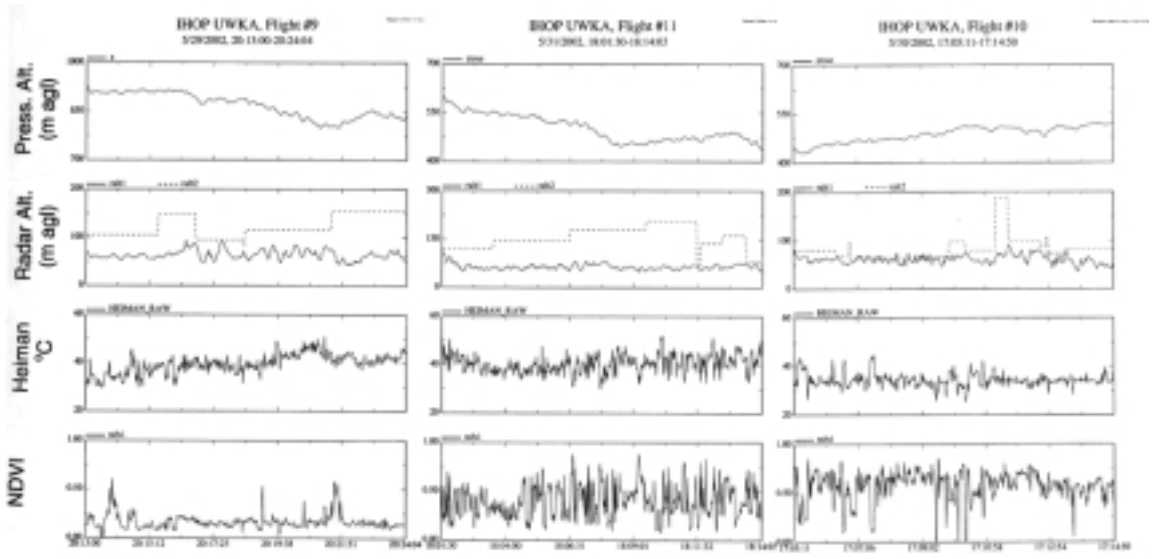

Fig. 3. Surface characteristics along each flight track based on representative 65-m agl flight legs. Left frame is for west (radar) flight track, center frame for the central flight track, and the right frame for the east flight track. Heiman oC denotes radiometric surface temperature. Horizontal axis is time (UTC).

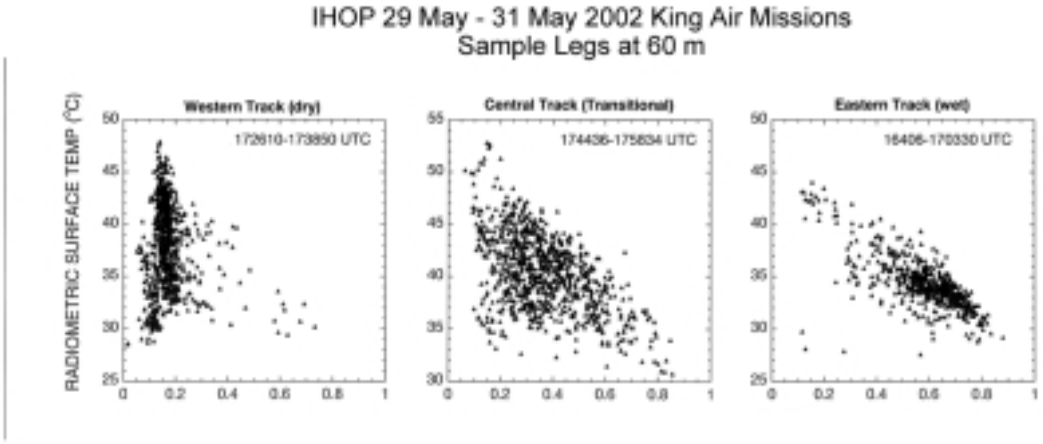

Fig. 4. Relationship of radiometric surface temperature and NDVI (horizontal axis) for the three tracks. Approximate rainfall totals for the NCAR ISFF surface stations along the corresponding track appear beneath.

REFERENCES

Alfieri, J., and P. Blanken, 2002: Relationship between NDVI and soil moisture over a sparse grassland canopy. 57th Annual Mtg, Rocky Mt. Hydrologic Research Center. 27 Sept. 2002, Boulder, Colorado.

Anthes, R.,1984: Enhancement of convective precipitation by mesoscale variations in vegetative covering in semiarid regions. *J. Clim. Appl. Meteor.*, **23**, 541-554.

Chen, F., and R. Avissar, 1994: The impact of land-surface wetness heterogeneity on mesoscale heat fluxes. *J. Appl. Meteor.*, **59**, 3751-3774.

Clark, T.L., t. Hauf, and J.P. Kuettner, 1986: Convective-forced internal gravity waves resulting from two-dimensional experiments. *Quart. J. Roy. Meteor. Soc.*, **112**, 899-926.

Krettenauer, K., and U. Schumann, 1989: Direct numerical simulation of thermal convection over a wavy surface. *Meteor. Atmos. Phys.*, **41**, 165-179.

LeMone, M.A., and Coauthors, 2000: Land-atmosphere interaction research and opportunities in the Walnut River watershed in southeast Kansas: CASES and ABLE. *Bull. Amer. Meteor. Soc.,* **81**, 757-780.

LeMone, M.A., and Coauthors, 2002: CASES-97: Late-morning warming and moistening of the convective boundary layer over the Walnut River watershed. *Bound.-Layer Meteor.*, **104**, 1-52.

Pielke, R.A., T.J. Lee, J.H. Copeland, J.L. Eastman, C.L. Ziegler, and C.A. Finley, 1997: Use of USGS-Provided data to improve weather and climate simulations. *Ecol. Appl.*, **7**, 3-21.

Segal, M., J.F.W. Purdom, J. Song, R.A. Pielke, and Y. Mahrer, 1986: Evaluation of cloud shading effects on the generation and modification of mesoscale circulations. *Mon. Wea. Rev.*, **114,** 1201-1212.

Segal, M., J.F. Weaver, J. Purdom, 1989: Some effects of the Yellowstone fire smoke on northeast Colorado at the end of summer. *Mon. Wea. Rev.,* **117**, 2278-2284.

Walko, R.L., W.R. Cotton, and R.A. Pielke, 1992: Large-Eddy Simulations of hilly terrain on the convective boundary layer. *Bound.-Layer Meteor.,* **58**, 133-150.

Weckwerth, T.M., and D.B. Parsons, 2003: An overview of the International H_2O Project (IHOP_2002). *Proc. Observing and Understanding the Variability of Water in Weather and Climate.* Amer. Meteor. Soc., Long Beach, CA, 9-13 Feb.

Yan, H., and R.A. Anthes, 1988: The effect of variations in surface moisture on mesoscale circulations. *Mon. Wea. Rev.*, **116**, 192-208.

Yates, E.N., and Coauthors, 2001: A CASES dataset for analyzing and parameterizing the effects of land-surface heterogeneity on averaged surface heat fluxes. *J. Appl. Meteor.*, **40**, 921-937.